water

Article

Assessing the Potential Impact of Rising Production of Industrial Wood Pellets on Streamflow in the Presence of Projected Changes in Land Use and Climate: A Case Study from the Oconee River Basin in Georgia, United States

Surendra Shrestha [1,2], Puneet Dwivedi [1,*], S. Kyle McKay [3] and David Radcliffe [4]

1 Warnell School of Forestry and Natural Resources, University of Georgia, Athens, GA 30602, USA; SurShrestha@clarku.edu
2 Graduate School of Geography, Clark University, Worcester, MA 01603, USA
3 U.S. Army Engineer Research and Development Center, New York, NY 10278, USA; Kyle.McKay@usace.army.mil
4 Department of Crop & Sciences, University of Georgia, Athens, GA 30602, USA; dradclif@uga.edu
* Correspondence: puneetd@uga.edu; Tel.: +1-706-542-2406

Received: 22 September 2018; Accepted: 8 January 2019; Published: 15 January 2019

Abstract: This study examines the impact of projected land use changes in the context of growing production of industrial wood pellets coupled with expected changes in precipitation and temperature due to the changing climate on streamflow in a watershed located in the northeastern corner of the Oconee River Basin. We used the Soil and Water Assessment Tool (SWAT) for ascertaining any changes in streamflow over time. The developed model was calibrated over a seven-year period (2001–2007) and validated over another seven-year period (2008–2014). Any changes in streamflow were simulated for a combination of 10 land use and climate change cases, from 2015 to 2028, under the two scenarios of High and Low Demand for industrial wood pellets. Our results suggest that streamflow is relatively stable (<1% change) for land use and temperature-related cases relative to the base case of no change in land use and climate. However, changes in precipitation by ±10% lead to considerable changes (±25%) in streamflow relative to the base case. Based on our results, expected changes in precipitation due to the changing climate will determine any changes in the streamflow, rather than projected land use changes in the context of rising demand for industrial wood pellets for export purposes in the selected watershed, keeping land under urban areas as constant. This study contributes to our broader understanding of the sustainability of the transatlantic industrial wood pellet trade; however, we suggest undertaking similar research at a larger spatial scale over a longer time horizon for understanding trade-offs across carbon, biodiversity, and water impacts of the transatlantic industrial wood pellet trade.

Keywords: wood pellets; land use change; climate change; hydrological modeling; SWAT

1. Introduction

The United States exported 4.6 million metric tons of industrial wood pellets in 2015, mostly to the European Union, including the United Kingdom [1]. It is expected that the export of industrial wood pellets will reach six million metric tons by 2020 [1], as European countries are increasingly utilizing solid biomass, including wood pellets, for replacing coal-based electricity for achieving the carbon reduction target under the 2020 Climate and Energy Package [2]. Currently, about 98% of exported industrial wood pellets are manufactured in the southern United States [3], a trend very likely to be continued in the near future, as southern states are the major producers of roundwood in the United States [4]. The growing demand for industrial wood pellets will increase forest cover in the southern United States [5] and, therefore, will affect the overall water balance in the region.

Several studies have examined the effect of changes in forest cover on watershed hydrology. Trimble et al. [6] studied the impact of reforestation on streamflow in 10 large populated river basins in Alabama, Georgia, and South Carolina, and found that an increase in forest cover decreased annual stream discharge between 4% and 21%. Cruise et al. [7] assessed the impact of land cover changes on the hydrology of 12 small watersheds of Alabama, Georgia, and Tennessee, showing that the movement of land from agriculture to forestry reduced streamflow over time. Isik et al. [8] predicted changes in daily streamflow in response to changing land use in 10 watersheds of Georgia and found that the average streamflow decreased with increasing forest cover. In contradiction to existing studies, Grace [9] reviewed the effects of active forest management on water yields and quality in watersheds located in 13 southern states and found that water yield increased in harvested sites due to a decreased evapotranspiration (ET) rate.

Some studies have combined land use change models with hydrological models to assess the impacts of land use changes on hydrology. For example, Choi and Deal [10] connected a cellular, dynamic, spatial urban growth model and a semi-distributed continuous hydrology model, using a Hydrological Simulation Program for ascertaining changes in streamflow in response to future urban growth in the United States. Zhang et al. [11] combined an integrated land use change model with a hydrological model to assess changes in local hydrology relative to historical and potential land cover changes in Southwest China. Wijesekara et al. [12] combined a land use cellular automata model with a hydrological model for assessing the impact of land use changes on hydrological processes in the Elbow River watershed in southern Alberta, Canada. Recently, Giri et al. [13] coupled an agent-based probabilistic land use change model with the Soil and Water Assessment Tool (SWAT) to investigate the consequences of urban growth on hydrological changes in a watershed (Raritan Basin) located in central New Jersey. Overall, these studies indicated that a rise in the urban area leads to an increase in streamflow over time.

Studies have combined land use and climate change models with hydrological models to assess the combined effect of changes in land use and climate on the hydrology of a watershed. LaFontaine et al. [14] used SLEUTH (a cellular automaton model of urban and other land class change) to project land use changes and combined the obtained results with a hydrological model (Precipitation-Runoff Modeling System) in the presence of climate change for the Apalachicola–Chattahoochee–Flint River Basin. Similarly, Pervez and Henebry [15] used SWAT to evaluate freshwater availability for the projected climate and land use changes in the Brahmaputra River Basin. Wagner et al. [16] projected land use changes in SLEUTH first, and then combined these projections in a dynamic setting with SWAT, with evolving temperature and precipitation for evaluating any changes in the hydrology of a local watershed in India. These studies suggest that any changes in precipitation coupled with increasing urban areas will affect the watershed hydrology.

Most existing studies evaluate the carbon benefits of electricity generated from imported industrial wood pellets from the southern United States [17,18] or biodiversity [19,20]. Existing studies focusing on the hydrological impacts of bioenergy feedstocks in the southern United States analyze mostly agriculture-based bioenergy feedstocks [21,22]. Only a few studies have evaluated the hydrological impacts of wood-based feedstock for bioenergy development in the region. For example, Griffiths et al. [23] reported that the forestry best management practices could protect stream quality from intensive loblolly pine (*Pinus taeda* L.) management for bioenergy development for the first three and a half years, by conducting a watershed-scale experiment on watershed located in the Upper Coastal Plain of the southeastern United States. Christopher et al. [24] reported an increase in streamflow by four percent when seven percent of loblolly plantation was converted to switchgrass in Tombigbee River watershed in the southeastern United States. To the best of our understanding, no study has so far analyzed the hydrologic consequence of potential land use changes due to the rising production of industrial wood pellets in the southeastern United States in the presence of changing climate. Therefore, the goal of this study is to assess the potential impacts of changing land use and climate on the hydrology, in general, and streamflow in particular, of a local watershed in the context of rising demand for industrial wood pellets in the southeastern United States. We hope that our results will help in developing a comprehensive understanding of the overall sustainability of the transatlantic wood pellet trade by bringing a fresh perspective of hydrology into consideration, apart from existing studies on carbon [17,18] and biodiversity [19,20].

2. Study Area

We delineated the selected watershed (2438.5 km^2) located within Oconee River Basin at the USGS (United States Geological Survey) Gage # 02218300 on the Oconee River near Penfield, GA (Figure 1). The watershed is in the Piedmont Ecoregion with mean slope and elevation of 4.36° (σ = 3.02°) and 248.2 m (σ = 45.48 m), respectively. Average annual rainfall is approximately 1230 mm, and the average mean annual temperature is 16.6 °C. In 2011, the land cover types present in the selected watershed were deciduous forests (34.8%), developed (21.5%), pasture/hay (21.1%), grassland (7.7%), and evergreen forest (7.6%) [25]. Between 2001 and 2011, the highest increase was observed for low-intensity development (26.3%), followed by open space development (17.6%). Similarly, the highest decrease was observed for the evergreen forest (12.6%) followed by deciduous forest (7.3%) and pasture/hay (6.9%) (Table 1). About 15.6%, 1.1%, and 0.1% of the total area under shrubland, grassland, and pasture/hay has moved into evergreen forest since 2001, highlighting the dynamics between pine forests and other land uses in the selected watershed. Furthermore, this watershed is a potential site for a wood pellet mill announced by E-Pellets in 2014.

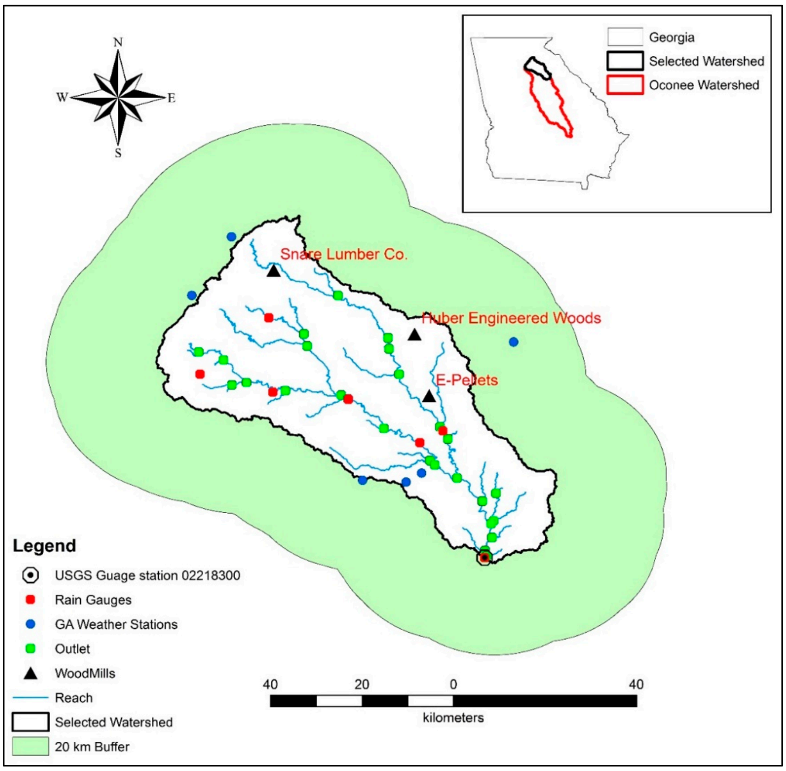

Figure 1. The selected watershed in the Oconee River Basin.

Table 1. Transition matrix showing the movement of land cover types (%) between 2001 and 2011 in the selected watershed.

Land Cover Class (Code)	Land Cover (km^2)		Land Cover (%)		Change (%) in Land Cover
	2001	2011	2001	2011	2001–2011
Open Water	16.5	17.2	0.7	0.7	4.2
Developed, Open Space	235.6	277	9.7	11.4	17.6
Developed, Low Intensity	138	174.3	5.7	7.1	26.3
Developed, Medium Intensity	28.1	56.5	1.2	2.3	101.2
Developed, High Intensity	9.6	15.9	0.4	0.7	65.6
Barren Land	19.8	14.8	0.8	0.6	−25.2
Deciduous Forest	914.2	847.6	37.5	34.8	−7.3
Evergreen Forest	214.3	187.2	8.8	7.7	−12.6
Mixed Forest	24.7	21.4	1	0.9	−13.4
Shrub/Scrub	5.7	33.2	0.2	1.4	482.5
Grassland/Herbaceous	188.9	188.3	7.7	7.7	−0.3
Pasture/Hay	553.1	514.8	22.7	21.1	−6.9
Cultivated Crops	2.1	2	0.1	0.1	−4.8
Woody Wetlands	87.3	85.4	3.6	3.5	−2.1
Emergent Herbaceous Wetlands	0.6	3	0	0.1	400

Source: U.S. Department of Agriculture/National Resource Conservation Service [25].

3. Method

SWAT provides a watershed modeling platform that predicts the impacts of land management on water quality and amount [26,27]. We used SWAT for ascertaining expected changes in the hydrology of the selected watershed, as it has been extensively used for runoff analysis [28,29], climate change effects on hydrological processes [30–32], and impact of any changes in land use on hydrology [32–36]. We developed a conceptual framework (Figure 2) for determining the potential impacts of changes in land use and climate on streamflow in the selected watershed using ArcSWAT (https://swat.tamu.edu/software/arcswat), an ArcGIS (www.arcgis.com), extension of SWAT.

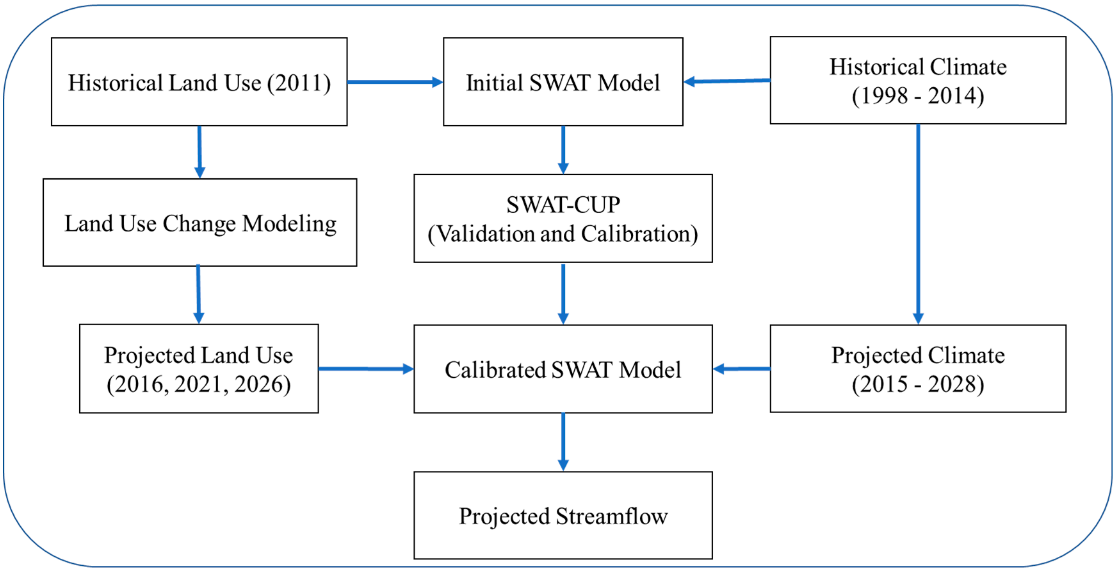

Figure 2. Conceptual modeling framework used for the modeling impact of changing land use and climate on the streamflow in the selected study area. SWAT-CUP—Soil and Water Assessment Tool-Calibration and Uncertainty Program.

3.1. Parameterization, Calibration, and Validation of SWAT

In SWAT, a watershed is divided into Hydrological Response Units (HRU) where each HRU is assumed to be homogenous in terms of soil, land use, and slope for the same hydrological response.

A water budget is then computed for each HRU based on precipitation, runoff, ET rate, percolation, and return flow [37] using a water balance equation by Arnold et al. [26], as shown below:

$$SW_t = SW_o + \sum_{i=1}^{t} (R_{day} - Q_{sur} - E_a - W_{seep} - Q_{gw}) \quad (1)$$

where SW_t (mm) is the final soil water content on day i, SW_o (mm) stands for the initial soil water content on day i, t is the time in days, R_{day} (mm) represents the amount of rainfall on day i, Q_{sur} (mm) is the amount of surface runoff on day i, E_a (mm) is the amount of ET on day i, W_{seep} (mm) is the amount of water entering the vadose zone from the soil profile on day i, and Q_{gw} (mm) depicts the amount of return flow on day i.

The SWAT model estimates surface runoff with the help of the Soil Conservation Service Curve Number (CN) equation by considering precipitation, topography, soil properties, land cover, and management [26,27]. The CNII value, CANMX (maximum canopy storage for each land use), and ALAI (initial leaf area index) are three important land use parameters in SWAT [34]. The SWAT model includes 102 different land use types in its land cover/plant growth database, each of which has a CNII value (curve number for antecedent soil moisture condition) assigned to it. The CN is a function of land use, soil's permeability, and antecedent soil moisture condition. The land use in the given watershed is assigned to one of those land use types in the model database. Based on the CNII value of each land use type, SWAT calculates the runoff from each land use type. Therefore, the success of the simulation depends on the accurate assignment of land use types [38]. The SCS Curve Number equation [39], estimating the amounts of runoff under varying land use and soil types in SWAT, is

$$Q_{surf} = \frac{\left(R_{day} - I_a\right)^2}{\left(R_{day} - I_a + S\right)} \quad (2)$$

where Q_{surf} is the accumulated runoff or rainfall excess, R_{day} is the rainfall depth for the day (mm H_2O), I_a is the initial abstractions which includes surface storage, interception, and infiltration prior to runoff (mm H_2O), and S is the retention parameter (mm H_2O). The retention parameter, S, is related to CN, which varies spatially because soils, land use, management, and slope all vary temporally, due to changes in soil water content. The retention parameter is given as

$$S = 25.4 \times \left(\frac{1000}{CN} - 10\right) \quad (3)$$

Vegetation characteristics affect hydrological processes, not only through their impact on surface runoff and recharge but also through their impact on canopy water storage and water use throughout the year. These vegetation impacts on the hydrological process are captured and reflected by several parameters like T_BASE, ALAI_MIN, BLAI, RDMX, CANMX, and EPCO [38]. We used default values for EPCO (plant uptake compensation factor) and CANMX. Leaf Area Index (LAI) is an important variable that controls the amount of precipitation reaching the soil, and the amount of ET lost from the canopy. In SWAT, LAI is estimated in the context of the plant growth model that lets plants develop a foliar mass until the maximum LAI (BLAI; 5 m^2/m^2 for pine and 4 m^2/m^2 for pasture/hay) has been reached. In the winter months, plants become dormant depending on base temperature (T_BASE) [27]. We used the lower base temperature, below which the crop is dormant, for pine (0 °C) compared to pasture/hay (12 °C). During dormancy, plants do not grow, and LAI is set to the minimum (ALAI_MIN; 0.75 m^2/m^2 for pine and 0 m^2/m^2 for pasture/hay). Also, we allowed pine to have a maximum root depth (RDMX) of 3.5 m compared to 2 m for pasture/hay. We have used the default value of SWAT parameters in this study, as they were within the range for land cover types in the Piedmont Region, based on our consultations with forestry and agricultural experts located in southern land-grant universities.

SWAT simulates potential evapotranspiration (PET) as a function of LAI and root depth, and it can be limited by soil moisture content. In SWAT, PET can be calculated with three options: The Penman–Monteith, Priestley–Taylor, and Hargreaves methods [27]. Based on our data, we used an improved version of the Hargreaves method for computing the PET in SWAT [40]:

$$\lambda E_0 = 0.0023 \times H_0 \times (T_{mx} - T_{mn})^{0.5} \times (T_{av} + 17.8) \quad (4)$$

where λ is the latent heat of vaporization (MJ kg^{-1}), E_o is the PET(mm day^{-1}), H_o is the extraterrestrial radiation (M m^{-2} day^{-1}), T_{mx} is the maximum air temperature for a given day (°C), T_{mn} is the minimum air temperature for a given day (°C), and T_{av} is the mean air temperature for a given day (°C). Once the PET was determined, the actual ET was calculated. SWAT first evaporates any rainfall stored in plant canopy by interception. Next, SWAT calculates the maximum amount of transpiration by plants and a maximum amount of sublimation/soil evaporation using an approach similar to Ritchie [41]. Once the maximum amount of sublimation/soil evaporation is calculated, SWAT removes water from the snowpack, if snow is present in the HRU, to meet the evaporative demand. When no snow is present in the HRU, evaporation from soil takes place [27].

We used the National Elevation Dataset to develop a Digital Elevation Model at a spatial resolution of 30 m [25]. We downloaded and used the SWAT/SSURGO soil database [42] for the analysis. SSURGO database contains information about soil as collected by the National Cooperative Soil Survey over the course of a century in the United States. We obtained land cover data from the National Land Cover Database [25] at a 30 m resolution. Weather data (mean precipitation, maximum temperature, and minimum temperature) were obtained from weather stations located within the 20 km buffer of the selected watershed. These weather stations are maintained by the University of Georgia Weather Network (www.weather.uga.edu).Finally, we obtained observed streamflow data from Penfield Gage Station (#02218300) for the calibration and the validation of the model. This Gage Station is maintained by the USGS (https://waterdata.usgs.gov/usa/nwis/uv?02218300).

Initial model parameters for simulations (Table 2) were selected from the literature [43–46]. We calibrated and validated the model using the SWAT Calibration and Uncertainty Program (CUP) 2012 (SWAT-CUP 2012), which allows for sensitivity analysis, calibration, validation, and uncertainty analysis by linking several optimization procedures to the SWAT [47]. We used the Sequential Uncertainty Fitting Version 2 (SUFI-2) algorithm for the calibration and validation of the SWAT model. During calibration, we allowed the model to "warm up" for 2 years and 10 months (1 March 1998 to 31 December 2000). For model calibration, we used monthly time steps for a seven-year period (1 January 2001 to 31 December 2007). During calibration, we removed the insensitive parameters at each iteration. We determined the sensitivity of a parameter based on p-value. We considered a parameter to be sensitive when its p-value is less than 0.05. After calibration, we ran the model for seven years (1 January 2008 to 31 December 2014), using the sensitive parameters from calibration for validation. Three measures of goodness-of-fit were applied: percent bias (PBIAS), correlation coefficient (R^2), and Nash–Sutcliffe (NS) model efficiency.

Table 2. Parameters used for the calibration of the SWAT model.

Parameter	Description	Fitted Value	*p*-Value
GW_DELAY	Time for water leaving the bottom of the root zone to reach the shallow aquifer (days)	158.8	0.8 **
GWQMN	Threshold depth of water in the shallow aquifer required for return flow to occur (mm)	576.9	<0.0001 ***
CH_K1	Effective hydraulic conductivity in tributary channel alluvium (mm/h)	9.1	0.15 *
CH_K2	Main channel hydraulic conductivity (mm/h)	0.8	<0.0001 ***
CH_N1	Manning's "n" value for tributary channels	0.3	0.53 *
CH_N2	Manning's "n" value for the main channel	0.1	0.001 ***
GW_REVAP	Groundwater re-evaporation coefficient	0.0	<0.0001 ***
REVAPMN	Threshold water depth in the shallow aquifer for "revap" (mm)	276.5	0.41 *
SOL_AWC	Available soil water capacity (mm H_2O/mm soil)	0.4	<0.0001 ***
SOL_K	Saturated hydraulic conductivity (mm/h)	0.7	<0.0001 ***
TRNSRCH	Fraction of transmission losses from the main channel that enter deep aquifer	0.3	<0.0001 ***
CN2	Curve number for moisture condition II	−0.2	0.22 *
ALPHA_BF	Baseflow recession constant	−0.1	0.95 *
ALPHA_BNK	Baseflow alpha factor for bank storage (days)	0.1	0.08 *
ESCO	Soil evaporation compensation factor	0.5	0.57 *
EPCO	Plant uptake compensation factor	0.3	0.23 *
GW_SPYLD	Specific yield of the shallow aquifer (m^3/m^3)	0.2	0.83 *
RCHRG_DP	Recharge to deep aquifer	0.1	0.28 *
SURLAG	Surface runoff lag coefficient	9.2	0.22 *

* Deleted after the second iteration, ** Deleted after the third iteration, *** Sensitive parameters.

3.2. Land Use Change Modeling

First, we estimated suitability of growing loblolly pine in each pixel present in the watershed by calculating suitability score at each pixel using a weighted combination of five factors (slope, distance from roads, distance from water, distance from urban areas, and distance from the existing evergreen forest). Then, we classified pixels into three suitability categories of low, medium, and high, based on natural breaks present in the suitability scores. Please see Shrestha and Dwivedi [48] for more details on the suitability modeling. Third, we determined the historical transition rates between 2001 and 2011 using the National Land Cover Database. We have only considered land use changes across evergreen forest, shrubland, grassland, and pasture/hay, keeping all other land uses constant over time. Including other land uses (e.g., urban areas) would have overshadowed the hydrological impacts related with the land moving into forestry and increased harvest rates due to the additional demand for industrial wood pellets, as the hydrological signature of urban lands is significant relative to other land uses [10–12,14]. We did not consider other land uses due to concerns regarding food-for-fuel and biodiversity protection.

We created two scenarios of industrial wood pellet demand: High and Low. We increased the historical transition rates by 10, 20, and 30 times for low, medium, and high suitability classes under the High Demand scenario, respectively. Similarly, we increased the historical transition rates by 5, 10, and 15 times for low, medium, and high suitability classes under the Low Demand scenario, respectively (Table 3). We used transition rules to allocate a total number of cells transitioning to the evergreen forest from other land covers between 2012 and 2026 for both wood pellet demand scenarios (Figure 3). We allocated transitioning cells from land cover grassland and pasture/hay to shrubland, based on the distance from the proposed site of the pellet mill. Similarly, we harvested existing evergreen forest stands based on their distances from the proposed site of the pellet mill under the assumption that forestlands located near to the wood pellet mill will be harvested first. We applied transition rules to the total number of transitioning cells for each year using an appropriate Visual Basic script in MS Excel to obtain land uses for 2016, 2021, and 2026 separately.

Table 3. Suitability classes under four land covers with their respective historical and future rate of change on an annual basis.

	Evergreen Forest			Shrubland			Grassland			Pasture/Hay		
	Past	**Future**		**Past**	**Future**		**Past**	**Future**		**Past**	**Future**	
Scenarios	-	High	Low	-	High	Low	-	High	Low	-	High	Low
High	0.21	6.15	3.08	0.86	0.86	0.86	0.07	2.04	1.02	0.006	0.18	0.09
Medium	0.14	2.72	1.36	0.69	0.69	0.69	0.04	1.96	0.98	0.008	0.16	0.09
Low	0.01	0.11	0.06	0.05	0.05	0.05	0.02	0.19	0.10	0.004	0.04	0.02

Source: Shrestha and Dwivedi [48].

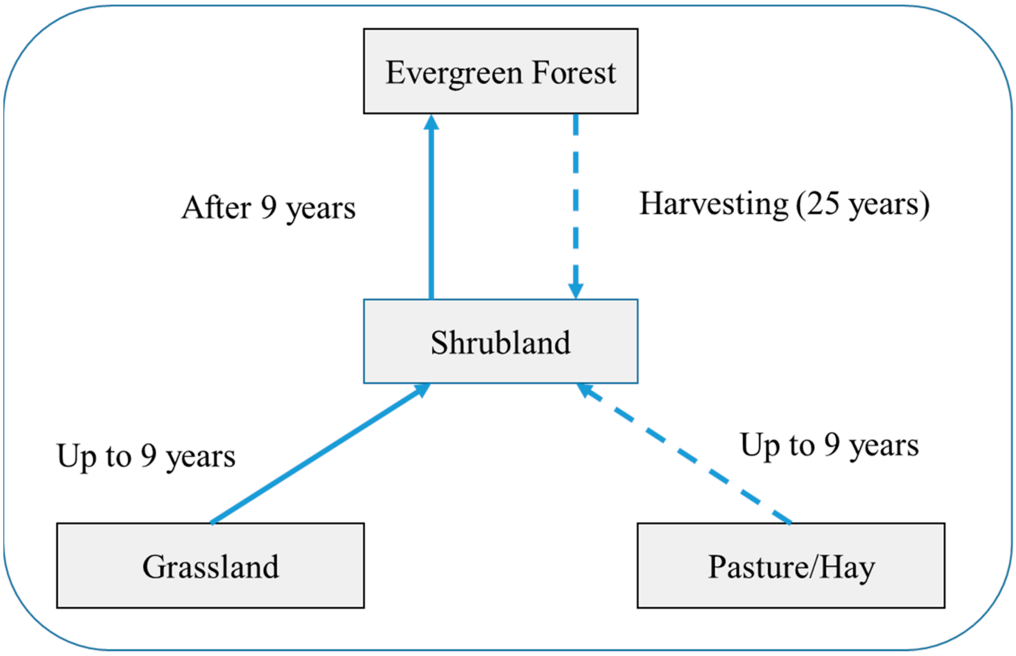

Figure 3. Transition rules between selected land covers in the watershed. A fixed number of pixels based on the transition rate from pasture/hay, grassland, and evergreen forest move to shrubland where they stay for the next nine years. After a nine-year period, they move to the evergreen forest where they stay until the harvest age of 25 years (a typical harvest age of loblolly pine in the southern United States) (source: Shrestha and Dwivedi [48]).

3.3. Ascertaining Changes in Climate

LaFontaine et al. [14] statistically downscaled three General Circulation Models (CCSM3, GFDL, and PCM) using an asynchronous regional regression model downscaling procedure to project maximum and minimum temperature and precipitation. Maximum and minimum daily temperatures were increased and ranged between 2.5 and 4 °C for IPCC high emission scenario and between 0.5 and 1.5 °C for the lower emission scenario. Similarly, CCSM3 and PCM-based simulations projected median precipitation to increase by about 10–15% for both emission scenarios, while GFDL-based simulation showed a median decrease of approximately 8% for the high emission scenario and an increase of approximately 3% for the low emission scenario. Based on LaFontaine et al. [14] and historical (1944–2015) meteorological data obtained from Ben Epps Climate Station located at the Athens/Ben Epps Airport in the selected watershed, 1 °C and 2 °C rise in temperature and ±10% change over the simulation period in precipitation were considered as representative climate change scenarios for the selected watershed. We simulated a combination of 10 land use and climate change cases to evaluate the effects of land use and climate change on the streamflow in the selected watershed (Table 4). We ran the base scenario without any changes in land cover and climate; the land use changes only scenarios with evolving land covers (2016, 2021, and 2026), climate change only scenarios with evolving precipitation and temperature, and combined scenarios with both evolving land covers and climate in SWAT for 14 years (1 January 2015 to 31 December 2028) under the scenarios of High and Low Demand for industrial wood pellets.

Table 4. Selected land use and climate change cases in this study. The base case is based on January 2001 to December 2014 climate with 2011 land use. PPT stands for precipitation.

Description	Abbreviation	Land Cover (Year)
Base	BAU	2011
Land use change only	LU	2016, 2021, 2026
Land use change, 1 °C temperature rise	LUCCT1+	2016, 2021, 2026
Land use change, 2 °C temperature rise	LUCCT2+	2016, 2021, 2026
Land use change, 10% PPT increase	LUCCP10+	2016, 2021, 2026
Land use change, 10% PPT decrease	LUCCP10−	2016, 2021, 2026
Land use change, 1 °C temperature rise, and 10% PPT increase	LUCCT1+P10+	2016, 2021, 2026
Land use change, 1 °C temperature rise, and 10% PPT decrease	LUCCT1+P10−	2016, 2021, 2026
Land use change, 2 °C temperature rise, and 10% PPT increase	LUCCT2+P10+	2016, 2021, 2026
Land use change, 2 °C temperature rise, and 10% PPT decrease	LUCCT2+P10−	2016, 2021, 2026

4. Results

4.1. Suitability Analysis

A total of 932 km^2 (38% area of the selected watershed) was taken into consideration for suitability analysis considering only four land cover classes of evergreen forest, shrubland, grassland, and hay/pasture. The high suitability sites were spatially clustered in the southern part of the watershed, due to their proximity to the existing evergreen forest area and to the announced pellet mill in the central part of the selected watershed (Figure 4). High, Medium, and Low suitability sites were 6.7% (162.5 km^2), 22.6% (548.5 km^2), and 8.6% (209.3 km^2) of the selected watershed (Table 5).

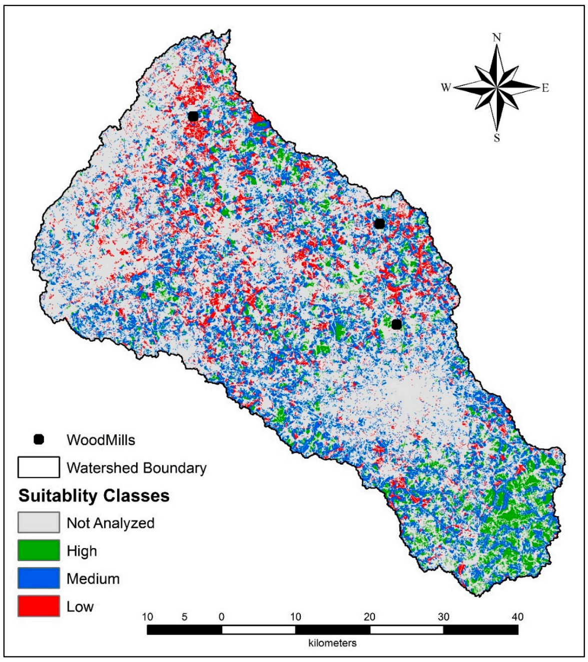

Figure 4. Suitability map of loblolly pine for selected watershed for selected land covers (evergreen forest, shrubland, grassland, and pasture/hay).

Table 5. Distribution of suitability classes under pasture/hay, grassland, shrubland, and evergreen forest.

Land Covers	Suitability Class (%)		
	High	Medium	Low
Evergreen Forest	2.7	4.9	0.1
Shrubland	0.6	0.6	0.1
Grassland	1.3	4.4	2.0
Pasture/Hay	2.1	12.6	6.4
Total %	6.7	22.6	8.6
Area (km^2)	162.5	548.5	209.3

4.2. Land Use Change

The spatial distribution of changed pixels shows that the changes occurred on pixels which were located near to the location of the announced pellet mill, as the allocation of pixels to the evergreen forest category is based on the distance from the announced pellet mill (Figure 5). In 2026, the total area occupied by evergreen forest, shrubland, grassland, and pasture/hay land cover classes was 7.1% (174.3 km^2), 3.9% (95.2 km^2), 6.2% (152.5 km^2), and 20.7% (600.0 km^2) of the total area of the watershed under the High Demand scenario, respectively. The area occupied by evergreen forest, shrubland, grassland, and pasture/hay land cover classes, in 2026, was −7.8%, 184.4%, −19.7%, and−1.86% for the corresponding land cover classes in 2011 under the High Demand scenario. We found that 41.7%, 9.9%, 20.6%, and 1.8% of evergreen forest, shrubland, grassland, and pasture/hay, originally present in 2011, moved across selected land covers by 2026, respectively, under the High Demand scenario (Figure 6). Similarly, under the Low Demand scenario, the total area occupied by evergreen forest, shrubland, grassland, and pasture/hay land cover classes was 7.3% (178.8 km^2), 2.8% (68.5 km^2), 6.9% (170 km^2), and 20.9% (514.7 km^2) of the total area of the selected watershed in 2026, respectively. The area occupied by evergreen forest, shrubland, grassland, and pasture/hay land cover classes in 2026 was −5.4%, 104.7%, −10.5%, and −0.9% for the corresponding land cover classes in 2011 under the Low Demand scenario, respectively. We found that 23.6, 9.9, 10.8, and 0.9% of evergreen forest, shrubland, grassland, and pasture/hay pixels originally present in 2011 moved across selected land covers by 2026 under the Low Demand scenario, respectively (Figure 7).

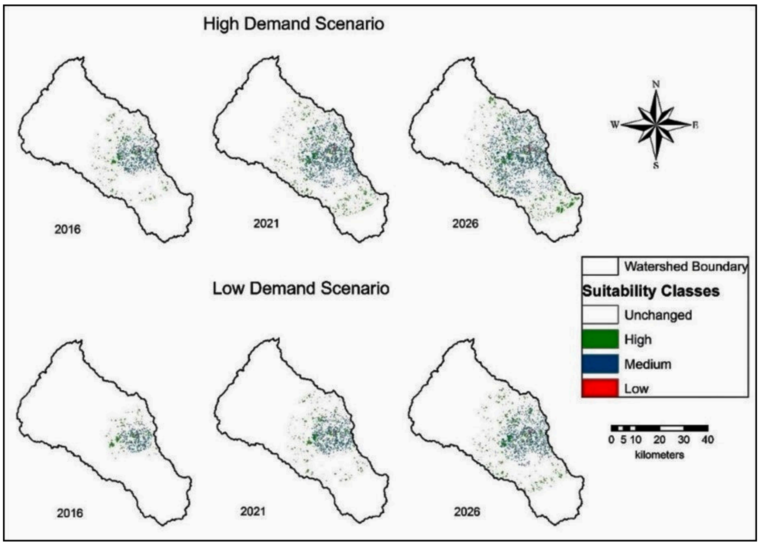

Figure 5. Projected land use under the scenarios of High and Low Demand for industrial wood pellets.: Shrestha and Dwivedi [48].

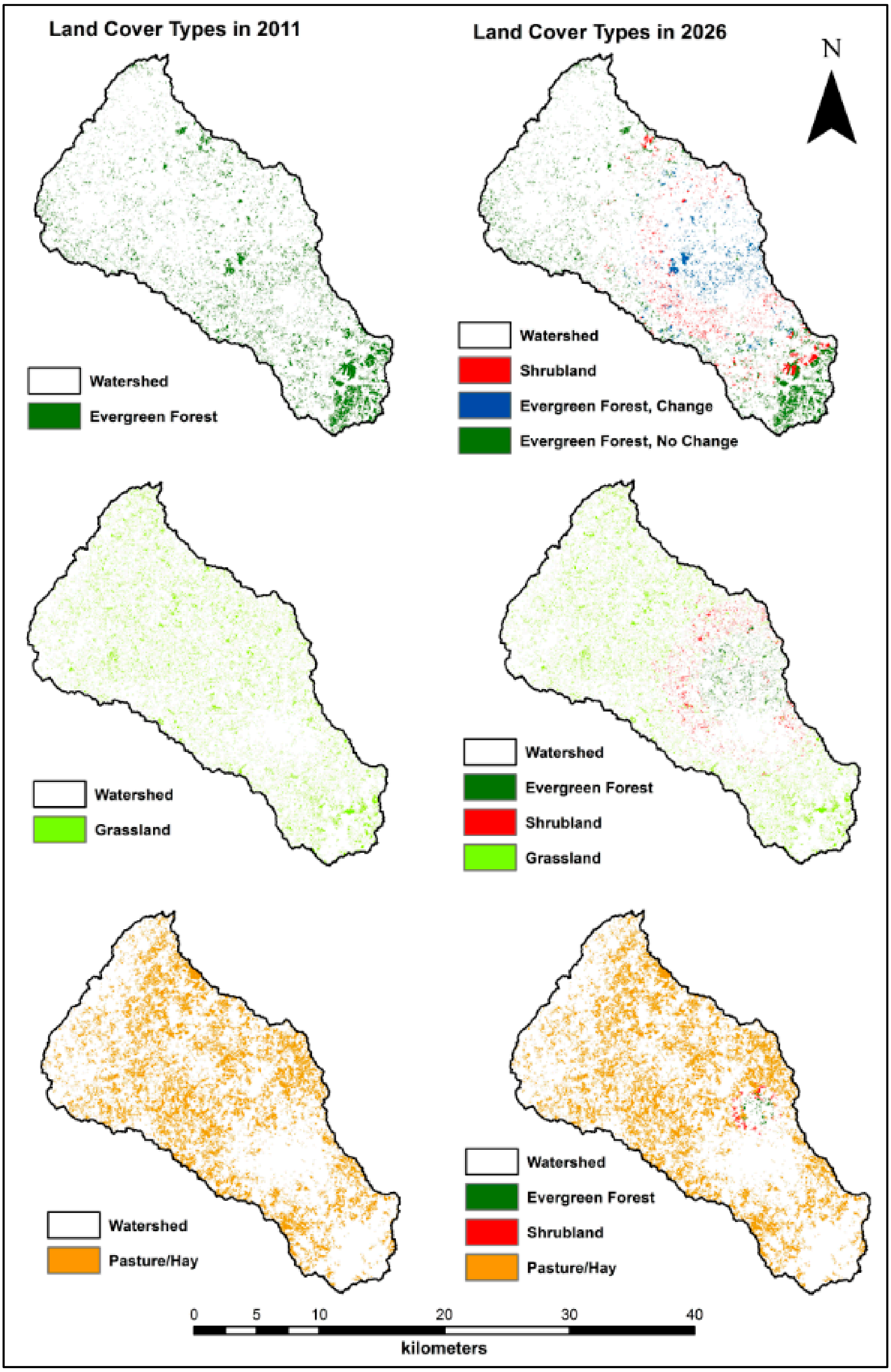

Figure 6. Transition of pixels to evergreen forest and shrubland over space and time under the High Demand scenario.

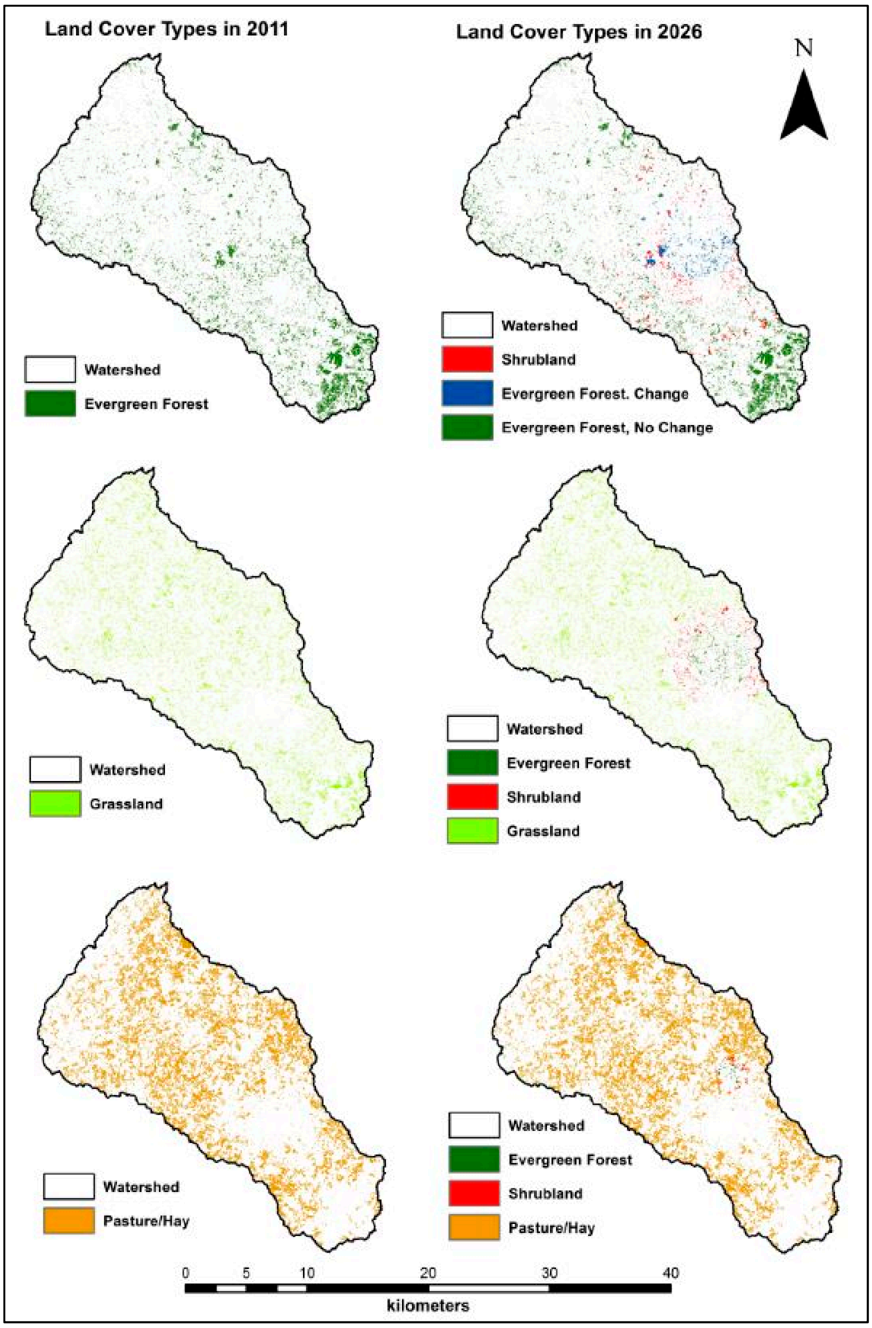

Figure 7. Transition of pixels to evergreen forest and shrubland over space and time under the Low Demand scenario.

4.3. SWAT Calibration and Validation

Initially, we calibrated 19 parameters pertaining to watershed hydrology in SWAT-CUP between January 2001 and December 2007. After the final iteration, only seven parameters (Table 2) were sensitive ($p < 0.001$). We obtained the values of PBIAS, NS, and R^2 for the SWAT simulations from SWAT-CUP using SUFI-2 algorithm (Table 6). According to Moriasi et al. [49], for a model fit for streamflow to be considered as satisfactory, the monthly NS value must be greater than 0.5. Our result showed a good fit for the SWAT simulation for both calibration and validation periods. The plots of the USGS observed streamflow, SWAT best simulation streamflow, and the 95% prediction uncertainty band for calibration and validation periods, respectively, are reported in Figure 8, further suggesting an overall good fit.

Table 6. Nash–Sutcliffe (NS) model efficiency coefficients, R^2, and percent bias (PBIAS) for calibration and validation relative to monthly averaged streamflow.

Simulation Period	Monthly Streamflow		
	NS	R^2	PBIAS (%)
2001–2007 (Calibration)	0.76	0.81	7.28
2008–2014 (Validation)	0.88	0.89	3.57
2001–2014 (Base Scenario)	0.77	0.84	4.24

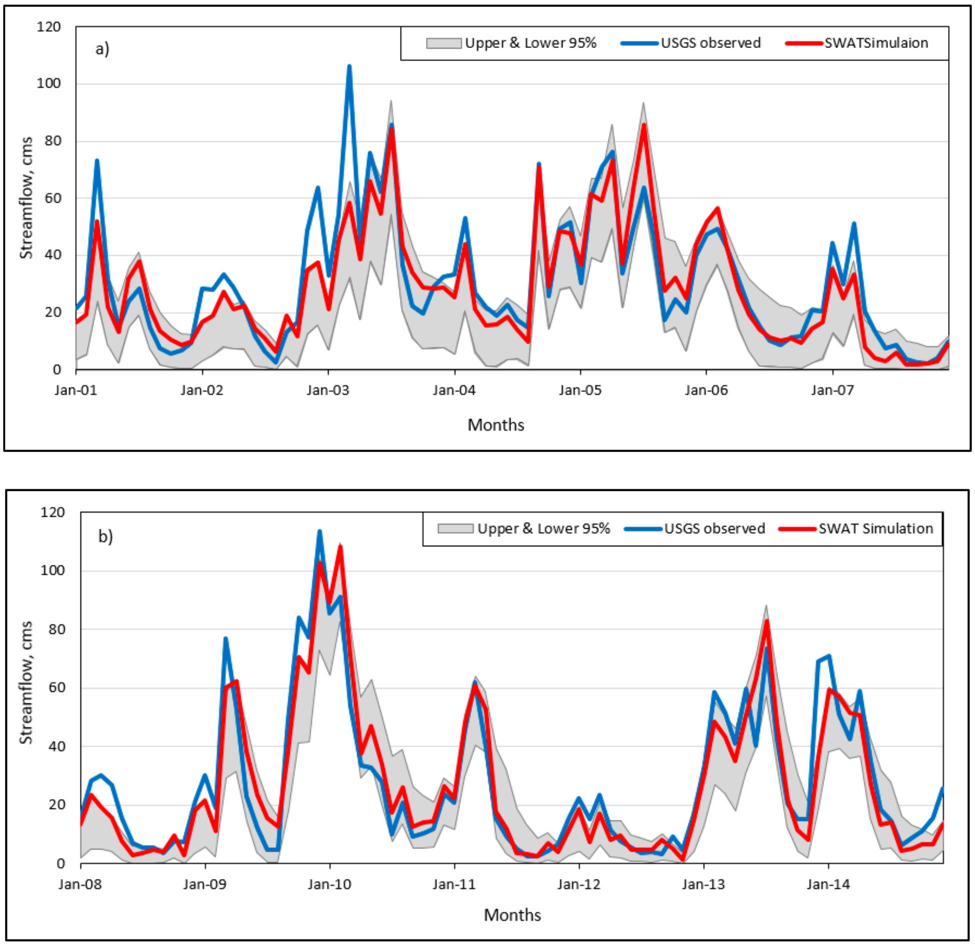

Figure 8. Trajectories of the observed USGS average monthly streamflow, SWAT best simulated average monthly streamflow, and upper and lower 95% prediction uncertainty band for (**a**) calibration period (January 2001 to December 2007) and (**b**) validation period (January 2008 to December 2014).

4.4. Land Use and Climate Change Impact on Streamflow

The average simulated streamflow under High and Low Demand scenarios for 10 cases (Table 7) suggested that changes in land use do not significantly affect streamflow. Compared to the base case, the streamflow increased by less than 1% under the High and Low Demand scenarios (Figure 9), indicating the low impact of land use change on streamflow. However, any changes in climate-related indicators, especially rainfall, significantly affected the streamflow. Streamflow under LUCCT1+ and LUCCT2+ decreased by about 0.8% and 0.9%, respectively (Figure 9) suggesting a little impact of any changes on streamflow with a rise in temperature. Under the cases related to the combined land use and climate changes, the highest increase in streamflow was under LUCCP10+, i.e., 26% and the utmost decrease was under LUCCT2+P10−, i.e., 25% for both demand scenarios.

Table 7. Simulated average streamflow with High and Low Demand scenarios for ten cases. Values in the brackets are percentage change relative to the base case. Streamflow units are in cubic meters per second (cms).

Cases	Land Use	Precipitation (mm)	Streamflow (cms) High Demand	Streamflow (cms) Low Demand
BAU	2011	1185.5	33.2	33.2
LU	2016	1185.5	33.3(0.3)	33.3(0.2)
	2021	1185.5	33.4(0.6)	33.3(0.2)
	2026	1185.5	33.4(0.6)	33.3(0.2)
LUCCT1+	2016	1185.5	32.9(−0.9)	32.9(−0.9)
	2021	1185.5	33(−0.6)	32.9(−0.9)
	2026	1185.5	34(−0.6)	32.9(−0.9)
LUCCT2+	2016	1185.5	32.9(−1.1)	32.8(−1.1)
	2021	1185.5	33(−0.8)	32.8(−1.1)
	2026	1185.5	33(−0.9)	32.8(−1.1)
LUCCP10+	2016	1303.6	41.6(25.2)	41.6(25.1)
	2021	1303.6	41.7(25.5)	41.6(25.2)
	2026	1303.6	41.7(25.5)	41.6(25.1)
LUCCP10−	2016	1066.1	25.2(−24.1)	25.2(−24.1)
	2021	1066.1	25.3(−23.8)	25.2(−24.1)
	2026	1066.1	25.3(−23.8)	26.4(−20.6)
LUCCT1+P10+	2016	1303.6	41.1(23.7)	41.1(23.7)
	2021	1303.6	41.2(24)	41.1(23.7)
	2026	1303.6	41.2(24)	41.1(23.6)
LUCCT2+P10+	2016	1303.6	40.9(23.1)	40.9(23)
	2021	1303.6	41(23.4)	40.9(23)
	2026	1303.6	42(23.4)	40.9(23)
LUCCT1+P10−	2016	1066.1	25(−24.6)	25(−24.8)
	2021	1066.1	25.1(−24.5)	25(−24.8)
	2026	1066.1	25.1(−24.5)	25(−24.9)
LUCCT2+P10−	2016	1066.1	25(−24.6)	25(−24.7)
	2021	1066.1	25.1(−24.4)	25(−24.7)
	2026	1066.1	25.2(−24.2)	25(−24.7)

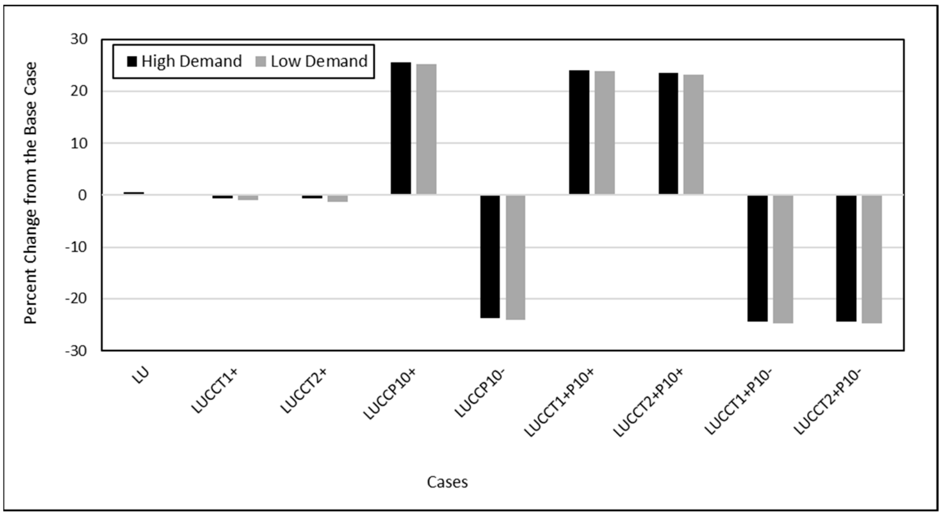

Figure 9. Changes in streamflow (%) with High and Low Demand scenarios for industrial wood pellets.

We also analyzed the impact of land use change on the streamflow at the sub-watershed level for both scenarios of High and Low Demand for industrial wood pellets in 2026 relative to 2011keeping climate constant. We found that the streamflow did not change in many sub-watersheds as the land cover was static in these sub-watersheds, mostly due to the absence of harvesting (Figure 10).

We also found that in all those sub-watersheds where harvesting took place, streamflow was higher in 2026, than in 2011, by a certain percentage point. This can be easily attributed to a decrease in ET between 2011 and 2026 (Figure 11) as the ET rate of a younger loblolly stand is lower than a mature stand [50–52]. Additionally, we noticed that the streamflow was higher in those sub-watersheds where land moved from grasslands and pasturelands to shrubland. Differences in ET for younger loblolly pine (before canopy closure) [50–52] and hay [53] in the southeastern region of the United States for the same soil types and climatic conditions could explain observed streamflow changes. Finally, we noticed that the streamflow decreased in only one sub-watershed (#35) between 2011 and 2026 under the High Demand scenario, and four sub-watersheds (#23, 29, 32, and 35) under the Low Demand scenario (Figure 10). This could be attributed to the fact that, in these sub-watersheds, harvesting took place during the early years of the simulation period; as a result, trees are mature by the end of 2026, and therefore have the same ET rate as that of a mature stand (Figure 11).

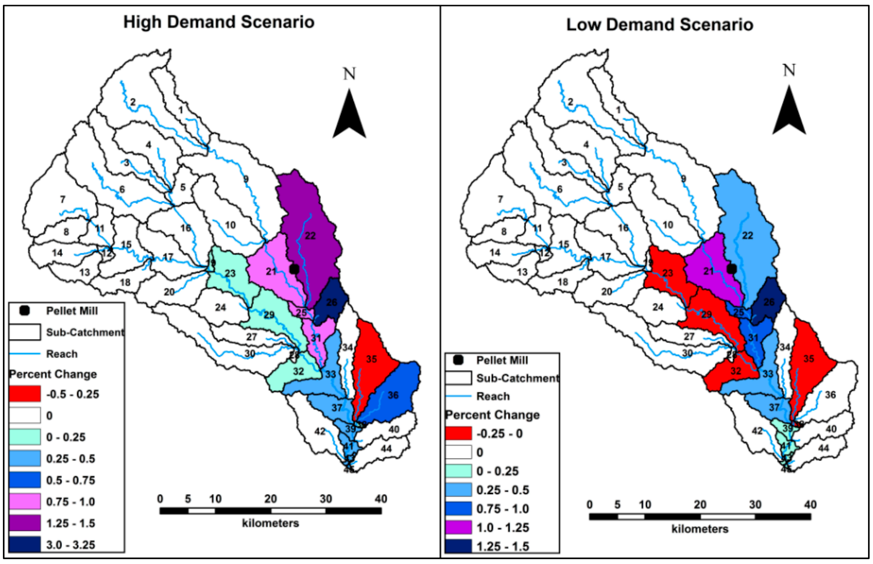

Figure 10. Change in streamflow under the High and Low Demand scenarios for industrial wood pellets at the sub-watershed level.

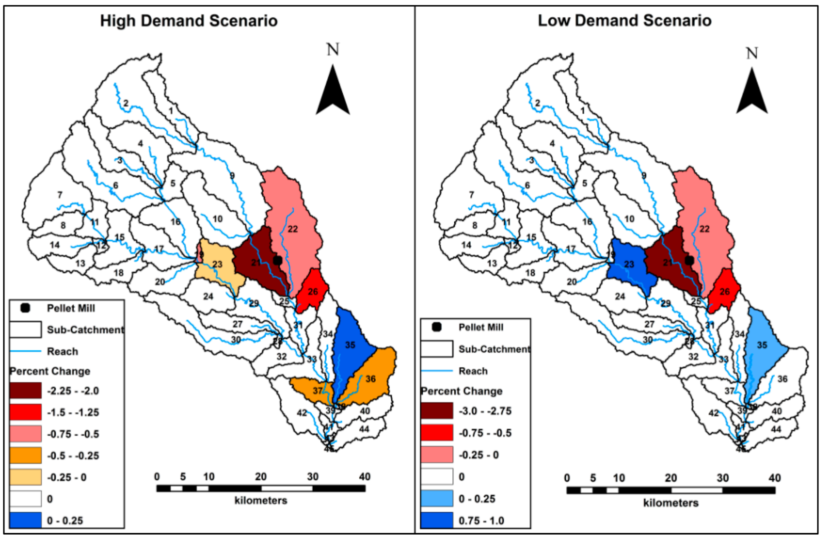

Figure 11. Percent change in evapotranspiration (ET) under the High and Low Demand scenarios for industrial wood pellets at the sub-watershed level.

5. Discussion

This study analyzes the potential impacts of projected land use and climate changes on the hydrology of a watershed located in the Oconee River Basin in the context of the growing demand for industrial wood pellets. To ascertain the hydrologic impacts of land use and climate changes, we used the SWAT model for 10different cases under the two scenarios of High and Low Demand for industrial wood pellets. Our results indicate that climate change, particularly, change in precipitation over the next two decades, would significantly affect the average streamflow in the selected watershed, instead of projected land use changes related to the increasing demand for industrial wood pellets in the southeastern United States.

Like other studies [8,14,32,33,54–59], this study found that land use change affects streamflow. Trimble et al. [6] reported a 4% to 21% decrease in the annual streamflow due to reforestation. Schoonover et al. [55] showed that the land use changes played a crucial role in driving the watershed hydrology. Our results reflect on such studies as we also found that land use change affects streamflow. However, these impacts were smaller relative to existing studies. This difference could be attributed to two reasons. First, most of the existing studies consider urban land cover changes within a selected watershed, whereas our study only considered land use changes across four land cover types (evergreen forest, shrubland, grassland, and pasture/hay). Additionally, we allowed the harvest of evergreen forests over time to meet the additional demand for wood pellets, which is typically not the case in other existing studies.

Our results suggest that climate change would significantly affect streamflow, as found in many of the previous studies [14,60–64]. The relative change in streamflow due to climate variability in this study was up to 26% in the cases with 10% increase in precipitation, and as much as −25% in the cases with 10% decrease in precipitation, which is relatively high compared to 5% to 13% reported by Hundecha and Bardossy [65], and 13% by Wang et al. [32]. However, some other studies have predicted a higher relative change in streamflow, such as 47% by Li et al. [60], 68% by Chen et al. [64], and between −65% and 114% by Niraula et al. [59]. Overall, the streamflow analysis found that the impact of climate variability on projected streamflow was relatively higher compared to the impact of land use change, a result which is consistent with the results of other studies [33,66]. Our results also suggest that the changes in precipitation would result in greater percent changes in streamflow relative to changes in temperature, which is consistent with Wang et al. [32].

We also noticed that streamflow went up by about 1%, even when the area under evergreen forest and shrubland went up by 1.9% and 1.0% in the selected watershed under the High and Low Demand for industrial wood pellets, respectively. This contradicts a general assumption which suggests that an increase in forest cover is inversely proportional to the streamflow [6–8] due to canopy interception of precipitation, increased infiltration capacity, and improved soil porosity, and increased ET. However, McLaughlin et al. [67] found that slash pine (*Pinus elliottii*) stands managed at lower basal areas can have up to 64% more cumulative water yield over a 25-year rotation, compared to systems managed for high-density timber production. Similarly, Sun et al. [68] found that water yield increased by 3%, 8%, and 13% when leaf area index was reduced by 20%, 50%, and 80%, respectively, while water yield decreased by 3% when leaf area index increased by 20% across 2100 large basins present in the coterminous United States. Additionally, Grace et al. [9] reported that water yields increased on harvested sites due to decreased ET by analyzing the literature across 13 southern states. These studies clearly indicate that an active forest management regime could modify a typical hydrological response associated with an increase in forest cover. Therefore, our results are consistent with our modeling assumptions as we are actively managing forested landscape for supplying roundwood to the pellet mill in this study.

6. Conclusions

We used SWAT for ascertaining the effect of potential changes in land use and climate on the hydrology of a watershed located in the Oconee River Basin. The calibrated SWAT model was run from

2015 to 2028, using a combination of 10 cases to simulate the response of streamflow to land use and climatic changes. The greatest increase and decrease in streamflow were found in the combined land use and climate change scenario, which accounts for 26% and 25%, respectively. Our results suggest that expected changes in climate will play a significant role in determining any changes in streamflow rather than expected land use changes in the context of the growing production of industrial wood pellets in the southeastern United States. We hope that this study will help us in developing a better understanding of the overall sustainability of the transatlantic wood pellet trade in the southeastern United States.

We suggest undertaking a similar study at a larger spatial scale for understanding trade-offs across carbon, biodiversity, and water impacts of the transatlantic industrial wood pellet trade. We also suggest running the model for a larger time frame for capturing the impact of temporal dynamics on streamflow. In this study, we have used default SWAT parameters for land cover types as they were within the range for the Piedmont Region. However, a future study could analyze changes in the streamflow relative to changes in the default parameters for developing a finer understanding about the impacts of changes in land use and climate on streamflow over large spatial scales and longer time horizons. Additionally, we have also not included the resulting changes in the productivity of evergreen forest due to changing climate, due to unavailability of the high-resolution land cover database. This could be coupled with changes in LAI over the stand age for developing a better understanding of potential changes in watershed hydrology, at the landscape level, over time. We expect that future studies will help in fulfilling these data and methodological gaps. We also hope that this study will be able to guide future studies appropriately.

Author Contributions: Conceptualization, P.D. and S.S.; Methodology, P.D., S.S., D.R. and S.K.M.; Formal Analysis, S.S.; Resources, P.D.; Writing—Original Draft Preparation, S.S. and P.D.; Writing—Review & Editing, P.D., S.S., S.K.M. and D.R.; Visualization, S.S.; Supervision, P.D. and D.R.; Project Administration, P.D.; Funding Acquisition, P.D.

Funding: This work is supported by the USDA National Institute of Food and Agriculture, McIntire Stennis project # GEOZ0192-MS.

Acknowledgments: Authors are thankful to Ian Flitcroft for providing access to weather data through the University of Georgia Weather Network.

Conflicts of Interest: Authors declare no conflict of interest related to the study.

References

1. Forisk. Wood Bioenergy Update and North American Pellet Capacity: Q3 2016. Available online: http://forisk.com/blog/2016/08/17/wood-bioenergy-update-north-american-pellet-capacity-q3-2016/ (accessed on 20 September 2017).
2. European Commission. 2020 Climate & Energy Package. Available online: http://ec.europa.eu/clima/policies/strategies/2020/index_en.htm (accessed on 10 March 2017).
3. Wong, P.; Bredehoeft, G.U.S. Wood Pellet Exports Double in 2013 in Response to Growing European Demand. 2014. Available online: http://www.eia.gov/todayinenergy/detail.cfm?id=16391 (accessed on 11 March 2017).
4. Oswalt, S.N.; Patrick, D.M.; Pugh, S.A.; Smith, W.B. *Forest Resources of the United States: A Technical Document Supporting the Forest Service 2020 update of the RPA Assessment*; USDA: Washington, DC, USA, 2018. [CrossRef]
5. Wang, W.; Dwivedi, P.; Abt, R.; Khanna, M. Carbon savings with transatlantic trade in pellets: Accounting for market-driven effects. *Environ. Res. Lett.* **2015**, *10*, 114019. [CrossRef]
6. Trimble, S.W.; Weirich, F.H.; Hoag, B.L. Reforestation and the reduction of water yield on the southern piedmont since CIRCA 1940. *Water Resour. Res.* **1987**, *23*, 425–437. [CrossRef]
7. Cruise, J.F.; Laymon, C.A.; Al-Hamdan, O.Z. Impact of 20 years of land-cover change on the hydrology of streams in the Southeastern United States. *J. Am. Water Resour. Assoc.* **2010**, *46*, 1159–1170. [CrossRef]
8. Isik, S.; Kalin, L.; Schoonover, J.E.; Srivastava, P.; Lockaby, B.G. Modeling effects of changing land use/cover on daily streamflow: An Artificial Neural Network and curve number based hybrid approach. *J. Hydrol.* **2013**, *485*, 103–112. [CrossRef]
9. Grace, J.M. Forest operations and water quality in the South. *Trans. ASAE* **2005**, *48*, 871–880. [CrossRef]

10. Choi, W.; Deal, B.M. Assessing hydrological impact of potential land use change through hydrological and land use change modeling for the Kishwaukee River basin (USA). *J. Environ. Manag.* **2008**, *88*, 1119–1130. [CrossRef] [PubMed]
11. Zhang, X.N.; Liu, Y.Y.; Fang, Y.H.; Liu, B.J.; Xia, D.Z. Modeling and assessing hydrologic processes for historical and potential land-cover change in the Duoyingping watershed, southwest China. *Phys. Chem. Earth* **2012**, *53–54*, 19–29. [CrossRef]
12. Wijesekara, G.N.; Gupta, A.; Valeo, C.; Hasbani, J.G.; Qiao, Y.; Delaney, P.; Marceau, D.J. Assessing the impact of future land-use changes on hydrological processes in the Elbow River watershed in southern Alberta, Canada. *J. Hydrol.* **2012**, *412–413*, 220–232. [CrossRef]
13. Giri, S.; Arbab, N.N.; Lathrop, R.G. Water security assessment of current and future scenarios through an integrated modeling framework in the Neshanic River Watershed. *J. Hydrol.* **2018**, *563*, 1025–1041. [CrossRef]
14. LaFontaine, J.H.; Hay, L.E.; Viger, R.J.; Regan, R.S.; Markstrom, S.L. Effects of climate and land cover on hydrology in the Southeastern US: Potential impacts on watershed planning. *J. Am. Water Resour. Assoc.* **2015**, *51*, 1235–1261. [CrossRef]
15. Pervez, M.S.; Henebry, G.M. Assessing the impacts of climate and land use and land cover change on the freshwater availability in the Brahmaputra River basin. *J. Hydrol. Reg. Stud.* **2015**, *3*, 285–311. [CrossRef]
16. Wagner, P.D.; Bhallamudi, S.M.; Narasimhan, B.; Kantakumar, L.N.; Sudheer, K.P.; Kumar, S.; Schneider, K.; Fiener, P. Dynamic integration of land use changes in a hydrologic assessment of a rapidly developing Indian catchment. *Sci. Total Environ.* **2016**, *539*, 153–164. [CrossRef] [PubMed]
17. Dwivedi, P.; Khanna, M.; Bailis, R.; Ghilardi, A. Potential greenhouse gas benefits of transatlantic wood pellet trade. *Environ. Res. Lett.* **2014**, *9*, 24007. [CrossRef]
18. Khanna, M.; Dwivedi, P.; Abt, R. Is forest bioenergy carbon neutral or worse than coal? Implications of carbon accounting methods. *Int. Rev. Environ. Resour. Econ.* **2017**, *10*, 299–346. [CrossRef]
19. Fletcher, R.J.; Robertson, B.A.; Evans, J.; Doran, P.J.; Alavalapati, J.R.R.; Schemske, D.W. Biodiversity conservation in the era of biofuels: Risks and opportunities. *Front. Ecol. Environ.* **2011**, *9*, 161–168. [CrossRef]
20. Gottlieb, I.G.W.; Fletcher, R.J.; Nuñez-Regueiro, M.M.; Ober, H.; Smith, L.; Brosi, B.J. Alternative biomass strategies for bioenergy: Implications for bird communities across the southeastern United States. *GCB Bioenergy* **2017**, *9*, 1606–1617. [CrossRef]
21. Zhong, J.; Yu, T.E.; Clark, C.D.; English, B.C.; Larson, J.A.; Cheng, C.L. Effect of land use change for bioenergy production on feedstock cost and water quality. *Appl. Energy* **2018**, *210*, 580–590. [CrossRef]
22. Keerthi, S.; Miller, S.A. Regional differences in impacts to water quality from the bioenergy mandate. *Biomass Bioenergy* **2017**, *106*, 115–126. [CrossRef]
23. Griffiths, N.A.; Jackson, C.R.; Bitew, M.M.; Fortner, A.M.; Fouts, K.L.; McCracken, K.; Phillips, J.R. Water quality effects of short-rotation pine management for bioenergy feedstocks in the southeastern United States. *For. Ecol. Manag.* **2017**, *400*, 181–198. [CrossRef]
24. Christopher, S.F.; Schoenholtz, S.H.; Nettles, J.E. Water quantity implications of regional-scale switchgrass production in the southeastern US. *Biomass Bioenergy* **2015**, *83*, 50–59. [CrossRef]
25. USDA/NRCS Geospatial Data Gateway. Geospatial Data Gateway. United States Department of Agriculture Natural Resources Conservation Service. Available online: https://gdg.sc.egov.usda.gov/ (accessed on 20 March 2017).
26. Arnold, J.G.; Srinivasan, R.; Muttiah, R.S.; Williams, J.R. Large area hydrologic modeling and assessment part I: Model development. *J. Am. Water Resour. Assoc.* **1998**, *34*, 73–89. [CrossRef]
27. Neitsch, S.L.; Arnold, J.G.; Kiniry, J.R.; Williams, J.R. *Soil and Water Assessment Tool Theoretical Documentation Version 2009*; Texas Water Resources InstituteTechnical Report No. 406; Texas A&M University System: College Station, TX, USA, 2011.
28. Arnold, J.G.; Allen, P.M.; Bernhardt, G. A comprehensive surface-groundwater flow model. *J. Hydrol.* **1993**, *142*, 47–69. [CrossRef]
29. Bingner, R.L. Runoff simulated from Goodwin Creek Watershed using SWAT. *Trans. ASAE* **1996**, *39*, 85–90. [CrossRef]
30. Eckhardt, K.; Ulbrich, U. Potential impacts of climate change on groundwater recharge and streamflow in a central European low mountain range. *J. Hydrol.* **2003**, *284*, 244–252. [CrossRef]
31. Van Liew, M.W.; Arnold, J.G.; Garbrecht, J.D. Hydrologic simulation on agricultural watersheds: Choosing between two models. *Trans. ASAE* **2003**, *46*, 1539–1551. [CrossRef]

32. Wang, S.; Kang, S.; Zhang, L.; Li, F. Modelling hydrological response to different land-use and climate change scenarios in the Zamu River basin of northwest China. *Hydrol. Process.* **2008**, *22*, 2502–2510. [CrossRef]
33. Ozturk, M.; Copty, N.K.; Saysel, A.K. Modeling the impact of land use change on the hydrology of a rural watershed. *J. Hydrol.* **2013**, *497*, 97–109. [CrossRef]
34. Ghaffari, G.; Keesstra, S.; Ghodousi, J.; Ahmadi, H. SWAT-simulated hydrological impact of land-use change in the Zanjanrood Basin, Northwest Iran. *Hydrol. Process.* **2010**, *24*, 892–903. [CrossRef]
35. Fohrer, N.; Haverkamp, S.; Frede, H.G. Assessment of the effects of land use patterns on hydrologic landscape functions: Development of sustainable land use concepts for low mountain range areas. *Hydrol. Process.* **2005**, *19*, 659–672. [CrossRef]
36. Baker, T.J.; Miller, S.N. Using the Soil and Water Assessment Tool (SWAT) to assess land use impact on water resources in an East African watershed. *J. Hydrol.* **2013**, *486*, 100–111. [CrossRef]
37. Lin, Z.L.; Radcliffe, D.E. Automatic calibration and predictive uncertainty analysis of a semidistributed watershed model. *Vadose Zone J.* **2006**, *5*, 248–260. [CrossRef]
38. Neitsch, S.L.; Arnold, J.G.; Kiniry, J.R.; Williams, J.R.; King, K.W. *SWAT Manual*; USDA, Agricultural Research Service and Blackland Research Center, Texas A&M University: College Station, TX, USA, 2002.
39. Soil Conservation Service. Section 4: Hydrology. In *National Engineering Handbook*; SCS: Washington, DC, USA, 1972.
40. Hargreaves, G.L.; Hargreaves, G.H.; Riley, J.P. Agricultural benefits for Senegal River Basin. *J. Irrig. Drain. Eng.* **1985**, *111*, 113–124. [CrossRef]
41. Ritchie, J.T. Model for predicting evaporation from a row crop with incomplete cover. *Water Resour. Res.* **1972**, *8*, 1204–1213. [CrossRef]
42. Texas A&M University and USDA–ARS. *SWAT: Soil and Water Assessment Tool*; Texas A&M University: College Station, TX, USA, 2015.
43. Van Liew, M.W.; Veith, T.L.; Bosch, D.D.; Arnold, J.G. Suitability of SWAT for the conservation effects assessment project: Comparison on USDA Agricultural Research Service watersheds. *J. Hydrol. Eng.* **2007**, *12*, 173–189. [CrossRef]
44. Cibin, R.; Sudheer, K.P.; Chaubey, I. Sensitivity and identifiability of stream flow generation parameters of the SWAT model. *Hydrol. Process.* **2010**, *24*, 1133–1148. [CrossRef]
45. Arnold, J.G.; Moriasi, D.N.; Gassman, P.W.; Abbaspour, K.C.; White, M.J.; Srinivasan, R.; Santhi, C.; Harmel, R.D.; van Griensven, A.; Van Liew, M.W.; et al. SWAT: Model use, calibration, and validation. *Trans. ASABE* **2012**, *55*, 1491–1508. [CrossRef]
46. Oliver, C.W.; Radcliffe, D.E.; Risse, L.M.; Habteselassie, M.; Mukundan, R.; Jeong, J.; Hoghooghi, N. Quantifying the contribution of on-site wastewater treatment systems to stream discharge using the SWAT model. *J. Environ. Qual.* **2014**, *43*, 539–548. [CrossRef]
47. Abbaspour, K.C. *Swat-Cup 2012: SWAT Calibration and Uncertainty Programs—A User Manual*; Eawag, Swiss Federal Institute of Aquatic Sciences and Technology: Dubendorf, Switzerland, 2014.
48. Shrestha, S.; Dwivedi, P. Projecting land use changes by integrating site suitability analysis with historic land use change dynamics in the context of increasing demand for wood pellets in the Southern United States. *Forests* **2017**, *8*. [CrossRef]
49. Moriasi, D.N.; Gitau, M.W.; Pai, N.; Daggupati, P. Hydrologic and water quality models: Performance measures and evaluation criteria. *Trans. ASABE* **2015**, *58*, 1763–1785.
50. Liu, X.; Sun, G.; Mitra, B.; Noormets, A.; Gavazzi, M.J.; Domec, J.C.; Hallema, D.W.; Li, J.; Fang, Y.; King, J.S.; et al. Drought and thinning have limited impacts on evapotranspiration in a managed pine plantation on the southeastern United States coastal plain. *Agric. For. Meteorol.* **2018**, *262*, 14–23. [CrossRef]
51. Domec, J.C.; Sun, G.; Noormets, A.; Gavazzi, M.J.; Treasure, E.A.; Cohen, E.; Swenson, J.J.; McNulty, S.G.; King, J.S. A comparison of three methods to estimate evapotranspiration in two contrasting loblolly pine plantations: Age-related changes in water use and drought sensitivity of evapotranspiration components. *For. Sci.* **2012**, *58*, 497–512. [CrossRef]
52. Sun, G.; Noormets, A.; Gavazzi, M.J.; McNulty, S.G.; Chen, J.; Domec, J.C.; King, J.S.; Amatya, D.M.; Skaggs, R.W. Energy and water balance of two contrasting loblolly pine plantations on the lower coastal plain of North Carolina, USA. *For. Ecol. Manag.* **2010**, *259*, 1299–1310. [CrossRef]
53. Carrow, R.N. Drought resistance aspects of turfgrasses in the southeast: Evapotranspiration and crop coefficients. *Crop Sci.* **1995**, *35*, 1685–1690. [CrossRef]
54. Booth, D.B.; Hartley, D.; Jackson, R. Forest cover, impervious-surface area, and the mitigation of stormwater impacts. *J. Am. Water Resour. Assoc.* **2002**, *38*, 835–845. [CrossRef]

55. Schoonover, J.E.; Lockaby, B.G.; Helms, B.S. Impacts of land cover on stream hydrology in the west Georgia piedmont, USA. *J. Environ. Qual.* **2006**, *35*, 2123–2131. [CrossRef] [PubMed]
56. Hurkmans, R.T.W.L.; Terink, W.; Uijlenhoet, R.; Moors, E.J.; Troch, P.A.; Verburg, P.H. Effects of land use changes on streamflow generation in the Rhine basin. *Water Resour. Res.* **2009**, *45*, W06405. [CrossRef]
57. Qi, S.; Sun, G.; Wang, Y.; McNulty, S.G.; Myers, J.A.M. Streamflow response to climate and landuse changes in a coastal watershed in North Carolina. *Trans. ASABE* **2009**, *52*, 739–749. [CrossRef]
58. Price, K.; Jackson, C.R.; Parker, A.J.; Reitan, T.; Dowd, J.; Cyterski, M. Effects of watershed land use and geomorphology on stream low flows during severe drought conditions in the southern Blue Ridge Mountains, Georgia and North Carolina, United States. *Water Resour. Res.* **2011**, *47*, W02516. [CrossRef]
59. Niraula, R.; Meixner, T.; Norman, L.M. Determining the importance of model calibration for forecasting absolute/relative changes in streamflow from LULC and climate changes. *J. Hydrol.* **2015**, *522*, 439–451. [CrossRef]
60. Li, Z.; Liu, W.; Zhang, X.; Zheng, F. Impacts of land use change and climate variability on hydrology in an agricultural catchment on the Loess Plateau of China. *J. Hydrol.* **2009**, *377*, 35–42. [CrossRef]
61. Christensen, N.S.; Wood, A.W.; Voisin, N.; Lettenmaier, D.P.; Palmer, R.N. The effects of climate change on the hydrology and water resources of the Colorado River basin. *Clim. Chang.* **2004**, *62*, 337–363. [CrossRef]
62. Novotny, E.V.; Stefan, H.G. Stream flow in Minnesota: Indicator of climate change. *J. Hydrol.* **2007**, *334*, 319–333. [CrossRef]
63. Harding, B.L.; Wood, A.W.; Prairie, J.R. The implications of climate change scenario selection for future streamflow projection in the Upper Colorado River Basin. *Hydrol. Earth Syst. Sci.* **2012**, *16*, 3989–4007. [CrossRef]
64. Chen, H.; Tong, S.T.Y.; Yang, H.; Yang, Y.J. Simulating the hydrologic impacts of land-cover and climate changes in a semi-arid watershed. *Hydrol. Sci. J.* **2015**, *60*, 1739–1758. [CrossRef]
65. Hundecha, Y.; Bardossy, A. Modeling of the effect of land use changes on the runoff generation of a river basin through parameter regionalization of a watershed model. *J. Hydrol.* **2004**, *292*, 281–295. [CrossRef]
66. Chen, J. Simulating the impacts of climate variation and land-cover changes on basin hydrology: A case study of the Suomo basin. *Sci. China Ser. D* **2005**, *48*, 1501. [CrossRef]
67. Mclaughlin, D.L.; Kaplan, D.A.; Cohen, M.J. Managing forests for increased regional water yield in the southeastern U.S. coastal plain. *J. Am. Water Resour. Assoc.* **2013**, *49*, 953–965. [CrossRef]
68. Sun, G.; Caldwell, P.V.; McNulty, S.G. Modelling the potential role of forest thinning in maintaining water supplies under a changing climate across the conterminous United States. *Hydrol. Process.* **2015**, *29*, 5016–5030. [CrossRef]

© 2019 by the authors. Licensee MDPI, Basel, Switzerland. This article is an open access article distributed under the terms and conditions of the Creative Commons Attribution (CC BY) license (http://creativecommons.org/licenses/by/4.0/).